[12] Tracking Individual Proteins in Living Cells Using Single Quantum Dot Imaging

By SÉBASTIEN COURTY, CÉDRIC BOUZIGUES, CAMILLA LUCCARDINI, MARIE-VIRGINIE EHRENSPERGER, STÉPHANE BONNEAU, and MAXIME DAHAN

Abstract

Single quantum dot imaging is a powerful approach to probe the complex dynamics of individual biomolecules in living systems. Due to their remarkable photophysical properties and relatively small size, quantum dots can be used as ultrasensitive detection probes. They make possible the study of biological processes, both in the membrane or in the cytoplasm, at a truly molecular scale and with high spatial and temporal resolutions. This chapter presents methods used for tracking single biomolecules coupled to quantum dots in living cells from labeling procedures to the analysis of the quantum dot motion.

Introduction

Developments in cell biology are increasingly driven by the emergence of new imaging techniques. Advances in fluorescence microscopy, which allow biological processes to be imaged in real time, have had a particularly significant impact. Progress in cell imaging has mainly stemmed from the advent of genetically encoded markers (Lippincott-Schwartz and Patterson, 2003; Tsien, 2005), which have unquestionably revolutionized the way proteins can be studied in live cells. Thanks to the green fluorescent protein (GFP) and its many variants, important mechanisms such as molecular diffusion, gene expression, protein–protein interactions, or cell signaling can now be detected optically (Lippincott-Schwartz and Patterson, 2003; Shav-Tal *et al*., 2004; Tsien, 2005). The need to analyze them quantitatively has spurred a large effort involving techniques from cell and molecular biology, biochemistry, physics, and computer science.

The imaging techniques based on fluorescent proteins, however, suffer from some limitations. First, the photodegradation of the probes limits the observation time. Second, the optical sensitivity is usually limited to the simultaneous detection of several molecules and does not truly reach the level of single molecules. New physical techniques have pushed the boundaries of detection by enabling the observation of individual biomolecules *in vitro* (Weiss, 1999) and *in vivo* (Harms *et al*., 2001; Iino *et al*.,

METHODS IN ENZYMOLOGY, VOL. 414

0076-6879/06 $35.00
DOI: 10.1016/S0076-6879(06)14012-4

2001; Schutz *et al.*, 2000; Seisenberg *et al.*, 2001; Ueda *et al.*, 2001). These experiments have already shown that SM measurements provide valuable information that remains hidden in conventional measurements.

The introduction of semiconductor quantum dots as biological markers represents a new step for single molecule detection in live cells (Jaiswal and Simon, 2004; Medintz *et al.*, 2005; Michalet *et al.*, 2005). Due to their remarkable brightness and superior photostability (compared to conventional dyes), quantum dots can be used as ultrasensitive fluorescent probes allowing long-term acquisition with a good signal-to-noise ratio (SNR). They render possible the investigation of cellular processes with high spatial and temporal resolutions at a truly molecular scale. The ultrasensitive imaging methods using quantum dots have already shown their potential for the study of membrane proteins in living cells (Dahan *et al.*, 2003) and open up exciting prospects for the study of many complex biological processes.

Semiconductor Quantum Dots as Biological Probes

By combining a relatively small size and unique photophysical properties (Fig. 1), quantum dots (QDs) present a high interest as detection probes for biological imaging (Bruchez *et al.*, 1998; Chan and Nie, 1998).

- QDs are small inorganic nanoparticles with a diameter comprised between 2 and 10 nm and composed of different semiconductor materials. Following their synthesis in organic solvent, they can be

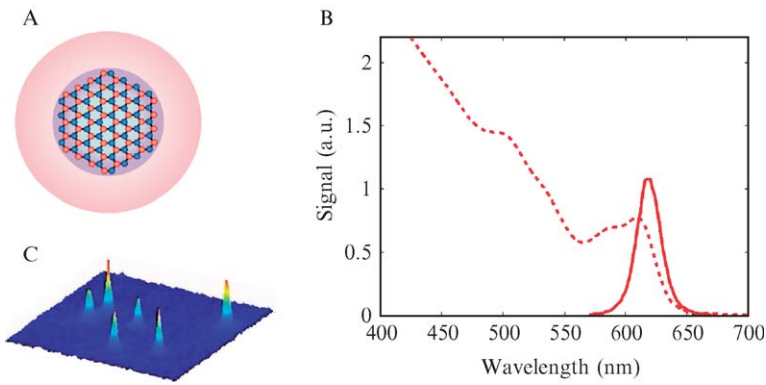

FIG. 1. (A) Structure of a functionalized quantum dot. The inorganic nanoparticle is covered by a layer of organic material used to solubilize and functionalize the QD, (B) absorption (dotted line) and emission spectra (plain line) of a QD sample, and (C) fluorescence image of single quantum dots deposited on a glass coverslip.

chemically modified for water solubilization and further functionalization (e.g., with Fab fragments or streptavidin).
- They possess both a large absorption and a narrow emission spectrum whose peak position is determined by the size of the semiconductor core and can be adjusted precisely during their synthesis by inorganic chemistry. As a consequence, QD samples with distinguishable emission wavelength can be excited with a single laser line, which make them ideal for multicolor detection (Wu *et al.*, 2003).
- Their photostability, which is far superior to that of conventional fluorophores (e.g., fluorescent proteins or organic dyes), overcomes the traditional limitation of photodegradation in fluorescent labeling.
- The synthesis and engineering of nanoparticles with different semiconductor materials and structures have expanded the range of possible emission wavelengths from the visible, ideally suited for immunofluorescence, to the red and infrared regions, more appropriate for imaging in tissues and animals (Kim *et al.*, 2004).

The potential of QDs as biological probes has now been demonstrated in many cases, and their applications, *in vitro* either in live cells or in organisms, are multiplying rapidly (Michalet *et al.*, 2005; Medintz *et al.*, 2005).

Single Molecule Imaging in Living Cells

A large choice of probes, such as fluorophores, quantum dots or beads, is now available to perform single molecule experiments in live cells. Selecting the right one depends on a number of physical and biochemical properties that should be evaluated for each system. Important factors are (i) the photostability, (ii) the extinction coefficient, (iii) the size, and (iv) the stoechiometry with which the detection probe can be bioconjugated to a biomolecule of interest (ideally, it should be achieved in a 1:1 ratio). A figure of merit, based on the value of these parameters for the different probes, is summarized in Table I.

For single molecule tracking, quantum dots are now probably the most favorable probe as they combine a relatively small size (radius $\sim$10 nm, including the surface organic groups) with a remarkable brightness and a superior photostability, allowing long-term acquisition with a good signal-to-noise ratio. The high SNR primarily comes from the extinction coefficient ε of the QDs, which is on the order of $10^6\ M^{-1}\ 1\ cm^{-1}$ in the visible, 10 to 100 times higher than that of standard organic fluorophores (dyes or GFP). This translates directly into the number of photons N detected for a single emitting QD in a given acquisition time τ:

TABLE I
FIGURE OF MERIT FOR DIFFERENT PROBES USED IN SINGLE MOLECULE TRACKING EXPERIMENTS

Probe	Size	Photostability	Extinction coefficient	Stoichiometry
Organic fluorophores (Cy3, Cy5, Alexi, etc.)	+++ 1 nm	+ ~1–10 s	++ $\sim 10^5$	++
GFP	++ 2–4 nm	− ~ 100 ms	+ $\sim 10^4$–10^5	+++
Quantum dots	+ ~10–20 nm	+++ >20 mn	+++ $\sim 10^6$	+
Beads	− 40 nm – 1 μm	∞	Scattered light	−

Photostability corresponds to the typical time during which a probe can be imaged continuously in a single molecule experiment. The extinction coefficient is expressed in $M^{-1}cm^{-1}l$. "Stoichiometry" is an indication of how easily a probe can be conjugated to a single biomolecule with a ratio of 1:1.

$$N = \alpha q \left(\frac{2303\varepsilon}{N_A}\right)\left(\frac{I\lambda}{hc}\right)\tau$$

where α is the detection efficiency ($\sim$0.1−5%), q is the QD emission quantum yield (ca. 30–80%), λ is the QD emission wavelength, h is the Planck constant (h = 6.63 10(−34) J.s), c is the speed of light, I is the excitation power per surface unit, and N_A is the Avogadro number. For the same input intensity I, one detects 10 to 100 times more fluorescence photons with a QD than with a fluorophore. With QDs, high values of N usually imply that the photon noise (also known as shot noise) is the primary source of noise in the detection system. It dominates other contributions, such as the background photon noise $\sigma = \sqrt{N}$ (due to scattered light and cellular autofluorescence), and the electronic noise (due to readout and dark current). In this context, the SNR:

$$SNR = \frac{N}{\sqrt{\sigma^2 + \sigma_b^2 + \sigma_e^2}} \approx \frac{N}{\sigma} \approx \sqrt{N}$$

Using seminconductor QDs as fluorescent probes, individual protein receptors have been tracked in the membrane of live neurons for durations longer than 20 min (Dahan *et al.*, 2003). This ultrasensitive imaging method has been extended to study the dynamics of single protein motors in living cells (Courty *et al.*, 2006). This chapter describes methods for tracking single biomolecules coupled to quantum dots in living cells, including

labeling procedures, optical microscopy setup and analysis of the QD motions.

Single Quantum Dot Tracking of Membrane Proteins

Understanding the structure and the dynamic organization of the plasma membrane is a major challenge in cell biology. To address these issues, single particle tracking is often considered a tool of choice, as it provides information with a spatial resolution on the order of 10 nm (see later), much higher than conventional confocal imaging; measuring the trajectories of single membrane molecules is therefore a way to directly probe the properties of the membrane with high spatial accuracy (Saxton and Jacobson, 1997).

In the fluid-mosaic model proposed by Singer and Nicolson (1972), the membrane is a homogeneous viscous fluid in which lipids and proteins undergo Brownian diffusion. Although this model has proven extremely fruitful in understanding some properties of the membrane, it is considered too simple. Nowadays, the membrane is often described as compartmentalized with obstacles (barriers, fences, pickets) hindering the free diffusion (Murase *et al.*, 2004). In addition, there has been active debate about the structure, the dynamics, and the role of small lipid-rich membrane microdomains, known as lipid rafts.

Single molecule tracking experiments have also been used to understand the membrane organization on a larger length scale. Several experiments have focused on the dynamics of receptors for neurotransmitters, either excitatory (Borgdorff and Choquet, 2002; Tardin *et al.*, 2003) or inhibitory (Dahan *et al.*, 2003; Meier *et al.*, 2001), as the lateral diffusion may play an important role in the regulation of the number of receptors at synapses. The first single QD tracking experiments were in fact performed on glycine receptors in live neurons (Dahan *et al.*, 2003), and a key point in these experiments was the ability to observe receptors in the synaptic cleft, a domain previously inaccessible when using micrometer-sized latex beads as labels (Borgdorff and Choquet, 2002; Meier *et al.*, 2001).

The following protocol is used to label individual membrane GABA receptors in cultured neurons. The concentrations of labeling reagents (primary and secondary antibodies, quantum dots) indicated correspond to conditions found appropriate in our experiments. For a different biological system, the immunolabeling conditions may vary depending on the antigens and the antibodies and should be adjusted accordingly. When testing for the right dilution, cells should be imaged in live conditions, as fixation might induce an additional autofluorescent background that would complicate the detection of individual QDs.

Solutions and Materials

Culture Reagents and Buffers

1. Minimum essential medium (MEM; Sigma-Aldrich Corp., St. Louis, MO)
2. Neurobasal medium supplemented with B27, glutamine (Invitrogen, Carlsbad, CA), and 25 μl antibiotics
3. L-15 medium (Invitrogen) supplemented (for a 30-ml final volume) with 15 μl antibiotics, 30 μl progesterone 10 μg/ml, and glucose to 3.6 μg/ml
4. B27 (Invitrogen) ready to use
5. Glutamine (Invitrogen) diluted in water to 200 m*M*
6. Poly-ornithine (Sigma-Aldrich Corp.)
7. Fetal veal serum (FVS) (Invitrogen)
8. Deoxyribonuclease (DNase) (Sigma-Aldrich Corp.)
9. Bovine serum albumin (Sigma-Aldrich Corp.)
10. Antibiotics: penicillin 10,000 UI and streptomycin 10,000 μg/ml (Invitrogen)
11. Glucose (Sigma-Aldrich Corp.)
12. Vectashield (Vector Laboratories, Burlingame, CA).
13. Phosphate-buffered saline (PBS) 10×: 80.06 g NaCl, 2.02 g KCl, 2.05 g KH_2PO_4, 23.3 g Na_2HPO_4 in 1 liter of deionized water
14. Incubation buffer: A 10% orthoboric acid solution (10 g of orthoboric acid dissolved in a 100-ml water solution adjusted to pH 8 and filtered on 0.22-μm pores) and a 10% bovine serum albumin solution are added to water in respective volume proportions of 1/40 and 1/5. In order to obtain a final osmolarity around 260 mOsm, compatible with live cells, the incubation buffer has to be supplemented with 15% in volume of 1.43 *M* sucrose.
15. Paraformaldehyde 4%: 1 g of paraformaldehyde is dissolved in 22.5 ml of magnetically agitated water at 80°. If solution remains unclear after agitation, a droplet of 1 *M* NaOH is added. Solution is then completed with 2.5 ml of PBS10× and stored at −20°.

Antibodies and Quantum Dots

1. Primary antibody against γ2 subunit of $GABA_A$ receptor raised in rabbit (Euromedex, Mundolsheim, France) at 0.6 mg/ml stored at −20° in deionized water
2. Fab fragment of biotinylated goat antirabbit (Fab-GaR-Biot) (Jackson Immunoresearch Laboratories, West Grove, PA) stored at −20° in 50-50 glycerol-water buffer at 0.5 mg/ml
3. Streptavidin-coated quantum dots (2 μM) emitting at 605 nm (Quantum Dots Corp., Hayward, CA) stored at 4°

Methods

Cells and Medium Preparation

1. Coverslips are coated with polyornithine for one night and for a few hours with L15 medium supplemented with FVS (5% in volume) and $NaHCO_3$ 7% (2.5% in volume) before cell plating. Spinal cords of E14 rat embryo are dissected in PBS-glucose, incubated for 15 min at 37° in 1 ml of PBS supplemented with 20 μl of trypsine-EDTA 2.5%, and smoothly dissociated in DNase supplemented L15 medium. Spinal neurons are then plated on coverslips at concentrations between 5×10^4/ml and 2×10^5/ml in B27-neurobasal medium and stored in sterile boxes in an incubator at 37° under 5% of CO_2 until use for quantum dot staining.

2. In order to work with neurons in ambient air, it is necessary to use a specific medium, referenced here as MEM-Air. MEM powder is diluted in 800 ml of water, which is then completed with 6 g glucose, 4.5 ml of $NaHCO_3$ 7%, and 10 ml HEPES and sterilized by filtration on 0.22-μm pores. MEM-Air is completed immediately before experiments with 3 ml of deionized water 1 ml B27, 500 μl natrium pyruvate, and 500 μl glutamine for a 50-ml final volume.

Labeling for Single Molecule Experiments

1. Remove a coverslip from the culture boxes. Place it on a surface maintained at 37° and incubate with 500 μl of MEM-Air.
2. Aspirate the medium and add 100 μl of primary antibody (anti-γ2, 1:100) on the coverslip for 10 min at 37°.
3. Discard the primary antibody and wash the sample three (or more) times in 500 μl MEM-air.
4. Add 100 μl of secondary antibody (Fab-GaR-Bio, 1:200) for 10 min at 37°.
5. Discard the secondary antibodies and rinse the sample three times in 500 μl MEM-air.
6. Prepare the quantum dots at 1:2000 to 1:10,000 in the incubation buffer.
7. Incubate the coverslip for 1 min with QDs and then wash at least five times in MEM-air to remove free QD remaining in solution.

Single Quantum Dot Tracking of Intracellular Proteins

The high sensitivity achieved in single molecule imaging of membrane proteins suggests that QDs could be employed to accomplish a more challenging task: tracking the motion of individual intracellular proteins. QDs have already been used successfully to visualize biological processes

in the cytoplasm of live cells but so far not at the single molecule level. For instance, QDs have been microinjected in Xenopus embryos (Dubertret *et al.*, 2002) in order to trace the cell lineage but the number of nanoparticles was superior to 10^9 per injected cell. Lidke *et al.* (2004) also used QD-tagged epidermal growth factor (EGF) to directly image the internalization of EGF receptors and the subsequent signaling pathways.

Reaching single molecule sensitivity in the imaging of intracellular biomolecules raises several difficulties and has been achieved in very few experiments. First, QDs have to enter the cell cytoplasm and reach their molecular target. Second, the fluorescence of individual QDs has to be detected in a noisy environment due to the autofluorescence of intracellular compartments and organelles. Finally, the motion in the cytosol is likely to be three dimensional compared to bidimensional diffusion in the membrane. It makes SM tracking more complex than in membrane experiments and will likely require new computational methods to extract and analyze trajectories from imaging data.

The following approach has been used successfully to image the motion of biotinylated kinesin motors coupled to QDs in the cytoplasm of living HeLa cells (Courty *et al.*, 2006). The protocol can be adapted easily to detect other intracellular biomolecules.

Solutions and Materials

Culture Reagents and Buffers

1. Hypertonic medium (Influx-pinocytic cell-loading reagent, Invitrogen)
2. Hypotonic medium (prepared by combining D-MEM medium, without serum, and sterile deionized water in a 6:4 ratio)
3. Air-MEM medium (D-MEM medium without phenol red, supplemented with 33 m*M* glucose, 2 m*M* glutamine, and 10 m*M* HEPES)
4. D-MEM medium (Gibco, Invitrogen, Carlsbad, CA) with 4500 mg/liter D-glucose, 110 mg/liter sodium pyruvate, and nonessential amino acids, without L-glutamine
5. Glucose (Sigma-Aldrich Corp.)
6. FVS (Invitrogen)
7. Glutamine (Invitrogen) diluted in water to 200 m*M*
8. Penicillin-streptomycin (Gibco, Invitrogen) contains 10,000 units of penicillin [base] and 10,000 μg of streptomycin [base]/ml utilizing penicillin G [sodium salt] and streptomycin sulfate in 0.85% saline
9. PBS 10×: 80.06 g NaCl, 2.02 g KCl, 2.05 g KH_2PO_4, 23.3 g Na_2HPO_4 in 1 liter of deionized water
10. Circular glass coverslips (18 mm, Karl Hecht KG, Sondheim, Germany)

Quantum Dots

1. Commercial streptavidin-coated quantum dots (2 μM stock) emitting at 655 nm (Quantum Dots Corp.) stored at 4°
2. MicroSpin SR-400 column (GE Health Care) stored at 4°

Methods

Purification of Quantum Dots Streptavidin Conjugates (QD-SAVs)

Commercial QD-SAVs emitting at 655 nm need to be purified from free avidin present in the stock solution as shown on the HPLC chromatogram (Fig. 2). QD-SAVs are purified from free avidin by using microSpin SR-400 columns, as described in the following procedure.

1. Resuspend the resin in the microspin by vortexing for a few minutes.
2. Loosen the cap one-fourth turn and snap off the bottom closure.
3. Place the microspin column in a 1.5-ml Eppendorf tube for support.
4. Prespin the column at 735g for 1 min.
5. Place the microspin column in a new 1.5-ml low-binding Eppendorf tube (LoBind). Remove and discard the cap.
6. Load the quantum dots solution slowly (e.g., 50 μl at 100 nM) to the top center of the resin, being careful not to disturb the bed. Check with an ultraviolet lamp.
7. Spin the column at 735g for 2 min, and collect the purified quantum dots in the low binding support tube.
8. Measure the new concentration of purified QD-SAVs with a spectrophotometer (extinction coefficient at 405 nm $= 5.7 \times 10^6\, M^{-1} \mid \mathrm{cm}^{-1}$.

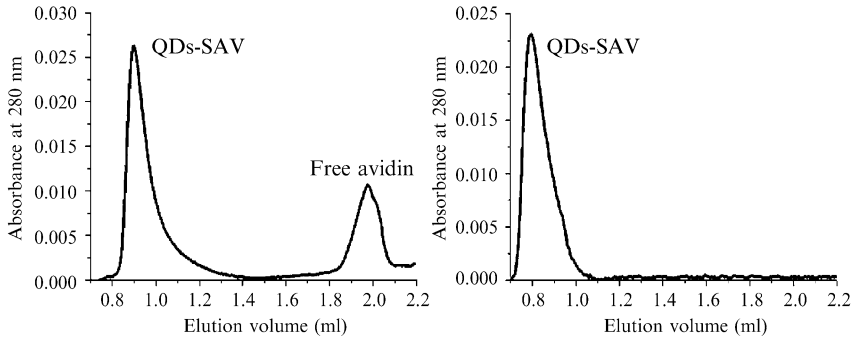

FIG. 2. Purification of quantum dots streptavidin conjugate. HPLC chromatograms of quantum dots streptavidin conjugate before (left) and after (right) purification on a microSpin SR-400 column.

Coupling of Biotinylated Proteins to QD-SAVs

For single molecule experiments, QD-SAVs are coupled at a final concentration of 1 n*M* with biotinylated proteins (ideally in a 1:1 ratio) in hypertonic solution for about 10 min at room temperature, before internalization in cultured cells. The hypertonic solution is prepared as described in the Invitrogen procedure (I-14402).

1. Prewarm 5 ml of D-MEM medium, without serum to 37°.
2. Melt the PEG (waxy solid on top of sucrose crystals) contained in the tube of influx-pinocytic cell-loading reagent by heating the tube in hot water (around 80°) for at least 2 min.
3. Remove the cap of the tube and quickly add 4.7 ml of 37° D-MEM medium without serum.
4. Replace the cap and vortex the tube vigorously to dissolve the sucrose crystals completely.
5. Once the solution is homogeneous, add 250 μl of serum and 50 μl of 1 *M* HEPES buffer, pH 7.4, in the tube.
6. Replace the cap and mix by vortexing the tube for a few minutes.

Internalization of QD-Protein Constructs in Live HeLa Cells

After coupling QD-SAVs to biotinylated proteins, the reaction product, QD-Ps, is loaded into live cells via a pinocytic process.

1. Cultured cells are plated at a density of 1.5×10^5 cells/cm^2 on 18-mm glass coverslips and maintained in D-MEM medium containing 10% fetal calf serum at 37° in a 5% CO_2 atmosphere.

2. Cells are incubated 10 min at 37° in the hypertonic medium along with QD-Ps.

3. After osmotic lysis of pinocytic vesicles, induce by incubating the cells at 37° for exactly 2 min in a hypotonic culture medium; QD-Ps are released homogeneously in the cell cytosol.

4. Cells are left for 10 min in Air-MEM medium before imaging. The osmotic lysis of pinocytic vesicles in the hypotonic solution does not alter the viability of cultured cells and does not result in lysosomal enzyme release. By comparison with other internalization techniques, such as microinjection, this method presents the main advantage that a large number of cells are loaded simultaneously in the same conditions.

Imaging of Single Conjugated Quantum Dot in Living Cells

Optical Microscope

The experiments are carried out using a standard inverted microscope (Olympus, IX71) mounted with an oil objective (Olympus $\times$ 60 NA = 1.4

PlanApo Ph3). An immersion objective should always be used with a numerical aperture of at least 1.2 and preferably 1.3 to 1.45. QDs are excited with a 100-W mercury lamp (excitation filter XF1074 525AF45, dichroic mirror DRLP 515, emission filters XF3304 605NB20 or 655WB20, Omega Opticals, Brattleboro, VT). Fluorescence images are collected with a Coolsnap ES (Roper Scientific) or a Peltier-cooled Micromax EB512FT CCD camera (Roper Scientific, Trenton, NJ). The pixel size p of the camera and the magnification M of the objective should be such that p/M is no larger than $\lambda/2\text{NA}$. In our case, $p = 13$ μm and $M = 60$ such that $p/M = 217$ nm. If p/M is too small, each individual spot will spread over too many pixels, leading to a decrease in SNR.

Calibration of the Optical System for Single Molecule Detection

To evaluate the ability of the optical system (objective, filter, camera) to detect individual quantum dots, a simple procedure can be followed.

1. Prepare a clean coverslip by rinsing it successively with methanol, acetone, and water. Dry it with clean compressed air or nitrogen.
2. Deposit a drop of QDs diluted at 1 nM in water. After 5–10 min, rinse with water and dry with clean compressed air or nitrogen.
3. Mount the coverslip on the microscope and focus on the surface. To facilitate focusing, a mark from a fluorescent pencil can be added on the proper side of the coverslip.
4. The signal of individual QDs corresponds to diffraction-limited spots and should be easily observable with the camera or in the eyepieces. The spots have a spatial extension given by $\lambda/2\text{NA}$. Individual QDs are identified by their fluorescence intermittency, that is, by the random succession of periods with high- and low-emission intensity.
5. If necessary, the blinking rate can be decreased by reducing the excitation intensity with a neutral density. As this will diminish the emission signal accordingly, a compromise should be found among detection sensitivity, acquisition time, and blinking.

Single Molecule Imaging in Live Cells

1. The coverslip is mounted on a cell chamber, maintained either at room temperature or at 37°.
2. By means of a phase-contract objective, select a zone of interest in a cell. This selection can be also achieved with less sensitivity with bright-field imaging.
3. Turn off the transmission light and turn on the fluorescence excitation. Individual spots can be detected with the camera or in the eyepieces. If necessary, refocus the microscope slightly.

4. A sequence of images can then be acquired (Figs. 3 and 4). In our experiments, we perform two different types of recordings: time lapse or streaming. In both cases, the excitation illumination is controlled by a computer-driven mechanical shutter. For streaming acquisition, the shutter is open permanently, allowing a continuous recording at an acquisition rate varying usually between 10 and 30 Hz. The maximum number of images in the sequence is determined by the storage space in the RAM or the hard drive of the computer. The acquisition rate is usually limited by the readout time of the camera and not by the brightness of the probe (single static QDs can be detected with 5 or 10 ms acquisition time).

5. The sequences of fluorescence contain fluorescence spots coming either from single QDs or from small aggregate. The blinking of QDs

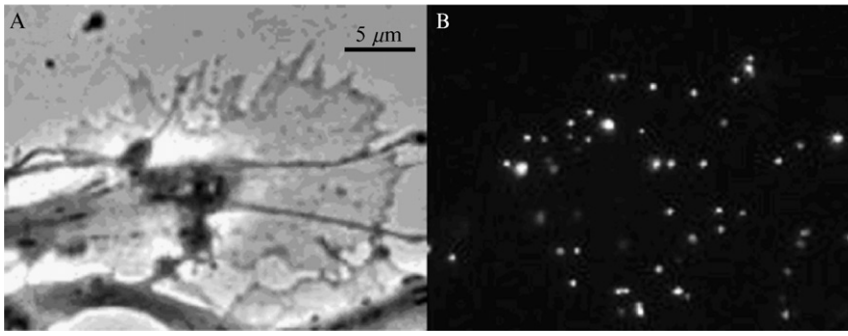

FIG. 3. Membrane labeling of single QDs in a nerve growth cone. (A: bright field image, B: fluorescence image).

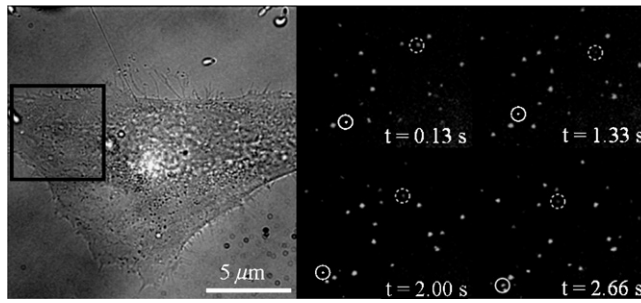

FIG. 4. Intracellular labeling of single QDs. (Left) Bright-field image of a HeLa cell in which QDs coupled to cytoplasmic proteins have been internalized. (Right) Tracking of individual biomolecules (two examples circled in plain and dashed lines) corresponding to the area marked on the left side.

provides a simple criterion to identify single molecules, as the probability for all the QDs forming an aggregate to simultaneously blink is small.

Data Processing

Acquisition of fluorescence image stacks is performed with MetaView (Universal Imaging, Downingtown, PA). Tracking and statistical analysis are carried out with custom-made software using Matlab (Mathworks, Natick, MA).

Analysis of Single QD trajectories

One of the main issues of single particle tracking experiments is extracting biological information from recorded trajectories. This section presents some of the techniques that have been used in order to measure quantities such as the diffusion coefficient or velocity.

Localization Accuracy of Single Quantum Dots

The value of the SNR has a direct consequence on the accuracy with which individual spots can be localized (Bobroff, 1986; Ober *et al*., 2004; Thompson *et al*., 2002; Yildiz *et al*., 2003). Because QDs are much smaller than the excitation wavelength $\lambda\sigma$, the shape of the fluorescence spots corresponds to the point spread function (PSF) of the optical system. Its width w is given by the optical resolution of the microscope, that is, $w \approx \lambda/(2*\mathrm{NA})$ where NA is the objective numerical aperture. For nanoparticles emitting around 600 nm and an oil-immersion objective with a NA of 1.3, this corresponds to about 230 nm. However, by fitting the PSF with a two-dimensional Gaussian curve, its center can be pinpointed with a much higher accuracy, on the order of w/SNR when the detection sensitivity is limited by the photon noise (Thomson *et al*., 2002). For SNR close to 30, as observed frequently with individual QD-tagged membrane receptors ($\tau \sim$ 50–100 ms), the accuracy can be as low as 5–10 nm.

Image Processing and Extraction of Single QD Trajectories

The technical details of our image processing method have been presented in Bonneau *et al*. (2004). Efficient tracking routines can also be found as plugins for imageJ (http://rsb.info.nih.gov/ij/).

Measurement of the Point Spread Function

Our method for the detection and tracking of quantum dots requires measurement of the PSF, which is the response of the optical system to a point source. Because quantum dots are much smaller than λ, they can be

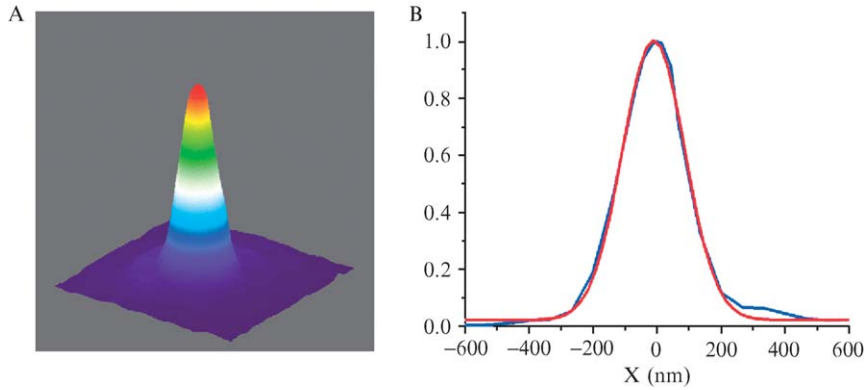

FIG. 5. (A) Experimental point spread function (PSF) of a single quantum dot. (B) The PSF (blue line) can be fitted by a Gaussian curve (red line) and its center can be localized with a high accuracy, on the order of λ/SNR.

reliably considered as a point source, and an image of a single QD is a good approximation of PSF (Fig. 5).

Detection of Spots

Fluorescent spots are detected on each frame of the stack by a method of correlation. A measure of similarity between real fluorescent image and the PSF (known from calibration images) is computed around local maxima of a small region of the fluorescence image. Correlation maxima, selected above a threshold depending on our estimation of the noise in the fluorescence image, reveal the position of QD-tagged molecules.

Individual Trajectories

Once QDs are detected on each frame, spots coming from the same QD have to be linked from frame to frame. Assuming that receptors are freely diffusing, we computed the probability for a spot, detected at a given position on a frame to be at another position on the following frame. The highest likelihood for a spot of the following frame provides the correct reconstruction of the trajectory. Spots of a given frame are then associated to the trajectory they are the most likely to belong to.

Blinking

Blinking brings additional difficulties for the tracking of single QDs, as the spots can disappear temporarily for random durations. A simple approach to account for blinking consists in computing continuous trajectories and then manually associating those corresponding to the same QD.

To reduce blinking rate, it is recommended to perform experiments with an excitation as low as possible.

Software

General tracking routines can be found as plugins for imageJ (http://rsb.info.nih.gov/ij/). We are currently implementing new tracking algorithms more suited for the emission properties of semiconductor QDs (Bonneau *et al.*, 2005). In the future, the corresponding software is intended to be freely available for potential users. More information can be found on our web site: http://www.lkb.ens.fr/recherche/optetbio/.

Mean Square Displacement Function

Once a trajectory $[x(t), y(t)]$ is determined, a way to extract physical information is the computation of $\rho(t)$, mean square displacement (MSD) (Saxton and Jacobson 1997). It is determined by the following formula

$$\rho(n\tau) = \frac{1}{N-n}\sum_{i=1}^{N-n}\left[\left(x((i+n)\tau) - x(i\tau)\right)^2 + \left(y((i+n)\tau) - y(i\tau)\right)^2\right]$$

where τ is the acquisition time and N is the total number of frames. Through computation of the MSD (Fig. 6), the nature of the molecular motions can be analyzed. A diffusive motion is revealed by a MSD varying linearly with a slope $4D$ (where D is the diffusion coefficient). In practice, the parameter D is obtained by fitting the first five points of the MSD with a linear curve. When an additional directed motion (with velocity v) is

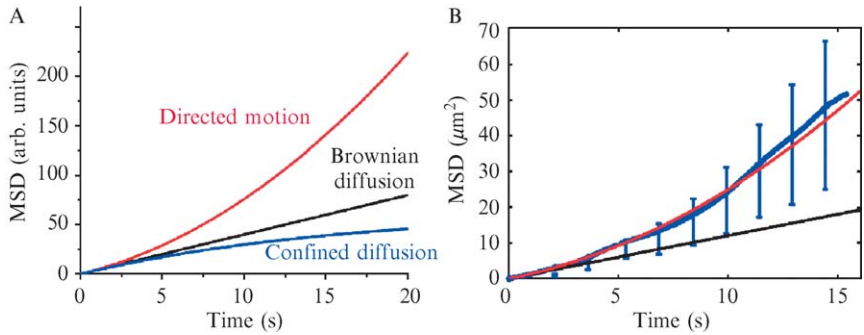

FIG. 6. (A) Theoretical curves of mean square displacement (MSD) as a function of time for directed (red line), Brownian (black line), and confined (blue line) motions. (B) Experimental MSD for a directed motion with velocity v and diffusion coefficient D. The red curve is a parabolic adjustment $4Dt + v^2t^2$ and the black linear curve corresponds to the initial slope $4Dt$.

present, $\rho(t)$ is in average equal to $4Dt + v^2t^2$. In the opposite, if the motion is confined, $\rho(t)$ should in average exhibit a negative curvature and saturate toward a finite value equal to the surface area explored during the movement.

Statistical Errors

Because the MSD is calculated on trajectories with a finite number of points, it is inherently affected by statistical errors. $s(\tau)$ the variance of $\rho(\tau)$ can be either estimated by computer simulations or, in the case of Brownian diffusion, computed by the following formula (Qian *et al*. 1991):

$$\sigma(\tau) = 4D\tau\left[(4n^2(N-n) + 2(N-n) + n - n^3)/6n(N-n)^2\right]^{1/2}$$

for $n \leq N/2$

$$\sigma(\tau) = 4D\tau\left[1 + \left((N-n)^3 - 4n(N-n)^2 + 4n - (N-n)\right)/6n^2(N-n)\right]^{1/2}$$

for $n \geq N/2$

Because $\sigma(\tau)$ increases rapidly with n, great care should be taken to account for these statistical fluctuations, especially when looking for deviation to simple Brownian diffusion (Qian *et al*., 1991).

Acknowledgments

We are grateful to A. Triller, S. Lévi, P. Rostaing, B. Riveau, C. Charrier, C. Hanus, L. Cohen, Y. Bellaiche, and G. Cappello for their contribution to the experiments and for many valuable discussions.

References

Bobroff, N. (1986). Position measurement with a resolution and noise limited instrument. *Rev. Sci. Instrum.* **57,** 1152–1157.

Bonneau, S., Cohen, L., and Dahan, M. (2004). A multiple target approach for single quantum dot tracking. *In* ''Proceedings of the IEEE International Symposium on Biological Imaging (ISBI 2004),'' p. 664.

Bonneau, S., Dahan, M., and Cohen, L. (2005). Single quantum dot tracking based on perceptual grouping using minimal paths in a spatio-temporal volume. *IEEE Transact. Image Proc.* **14,** 1384–1395.

Borgdorff, A. J., and Choquet, D. (2002). Regulation of AMPA receptor lateral movements. *Nature* **417,** 649–653.

Bruchez, M., Jr., Moronne, M., Gin, P., Weiss, S., and Alivisatos, A. P. (1998). Semiconductor nanocrystals as fluorescent biological labels. *Science* **281,** 2013–2016.

Chan, W. C., and Nie, S. (1998). Quantum dot bioconjugates for ultrasensitive nonisotopic detection. *Science* **281,** 2016–2018.

Courty, S., Luccardini, C., Bellaiche, Y., Cappello, G., and Dahan, M. (2006). Single quantum dot imaging of kinesin motors in living cells. **6**(7), 1491–1495.

Dahan, M., Levi, S., Luccardini, C., Rostaing, P., Riveau, B., and Triller, A. (2003). Diffusion dynamics of glycine receptors revealed by single-quantum dot tracking. *Science* **302,** 442–445.

Dubertret, B., Skourides, P., Norris, D. J., Noireaux, V., Brivanlou, A. H., and Libchaber, A. (2002). *In vivo* imaging of quantum dots encapsulated in phospholipid micelles. *Science* **298,** 1759–1762.

Harms, G. S., Cognet, L., Lommerse, P. H., Blab, G. A., Kahr, H., Gamsjager, R., Spaink, H. P., Soldatov, N. M., Romanin, C., and Schmidt, T. (2001). Single-molecule imaging of l-type Ca2+ channels in live cells. *Biophys. J.* **81,** 2639–2646.

Iino, R., Koyama, I., and Kusumi, A. (2001). Single molecule imaging of green fluorescent proteins in living cells: E-cadherin forms oligomers on the free cell surface. *Biophys. J.* **80,** 2667–2677.

Jaiswal, J. K., and Simon, S. M. (2004). Potentials and pitfalls of fluorescent quantum dots for biological imaging. *Trends Cell Biol.* **14,** 497–504.

Kim, S., Lim, Y. T., Soltesz, E. G., De Grand, A. M., Lee, J., Nakayama, A., Parker, J. A., Mihaljevic, T., Laurence, R. G., Dor, D. M., Cohn, L. H., Bawendi, M. G., and Frangioni, J. V. (2004). Near-infrared fluorescent type II quantum dots for sentinel lymph node mapping. *Nature Biotechnol.* **22,** 93–97.

Lippincott-Schwartz, J., and Patterson, G. H. (2003). Development and use of fluorescent protein markers in living cells. *Science* **300,** 87–91.

Medintz, I. L., Uyeda, H. T., Goldman, E. R., and Mattoussi, H. (2005). Quantum dot bioconjugates for imaging, labeling and sensing. *Nature Mater.* **4,** 435–446.

Meier, J., Vannier, C., Serge, A., Triller, A., and Choquet, D. (2001). Fast and reversible trapping of surface glycine receptors by gephyrin. *Nature Neurosci.* **4,** 253–260.

Michalet, X., Pinaud, F. F., Bentolila, L. A., Tsay, J. M., Doose, S., Li, J. J., Sundaresan, G., Wu, A. M., Gambhir, S. S., and Weiss, S. (2005). Quantum dots for live cells, *in vivo* imaging, and diagnostics. *Science* **307,** 538–544.

Murase, K., Fujiwara, T., Umemura, Y., Suzuki, K., Iino, R., Yamashita, H., Saito, M., Murakoshi, H., Ritchie, K., and Kusumi, A. (2004). Ultrafine membrane compartments for molecular diffusion as revealed by single molecule techniques. *Biophys. J.* **86,** 4075–4093.

Ober, R. J., Ram, S., and Ward, E. S. (2004). Localization accuracy in single-molecule microscopy. *Biophys. J.* **86,** 11185–11200.

Qian, H., Sheetz, M. P., and Elson, E. L. (1991). Analysis of diffusion and flow in two-dimensional systems. *Biophys. J.* **60**(4), 910–921.

Saxton, M. J., and Jacobson, K. (1997). Single-particle tracking: Applications to membrane dynamics. *Annu. Rev. Biophys. Biomol. Struct.* **26,** 373–399.

Schutz, G. J., Kada, G., Pastushenko, V. P., and Schindler, H. (2000). Properties of lipid microdomains in a muscle cell membrane visualized by single molecule microscopy. *EMBO J.* **19,** 892–901.

Seisenberger, G., Ried, M. U., Endress, T., Buning, H., Hallek, M., and Brauchle, C. (2001). Real-time single-molecule imaging of the infection pathway of an adeno-associated virus. *Science* **294,** 1929–1932.

Shav-Tal, Y., Singer, R. H., and Darzacq, X. (2004). Imaging gene expression in single living cells. *Nature Rev. Mol. Cell. Biol.* **5,** 855–861.

Singer, S. J., and Nicolson, G. L. (1972). The fluid mosaic model of the structure of cell membranes. *Science* **175,** 720–731.

Tardin, C., Cognet, L., Bats, C., Lounis, B., and Choquet, D. (2003). Direct imaging of lateral movements of AMPA receptors inside synapses. *EMBO J.* **22,** 4656–4665.

Thompson, R. E., Larson, D. R., and Webb, W. W. (2002). Precise nanometer localization analysis for individual fluorescent probes. *Biophys. J.* **82,** 2775–2783.

Tsien, R. Y. (2005). Building and breeding molecules to spy on cells and tumors. *FEBS Lett.* **579,** 927–932.

Ueda, M., Sako, Y., Tanaka, T., Devreotes, P., and Yanagida, T. (2001). Single-molecule analysis of chemotactic signaling in Dictyostelium cells. *Science* **294,** 864–867.

Yildiz, A., Forkey, J. N., McKinney, S. A., Ha, T., Goldman, Y. E., and Selvin, P. R. (2003). Myosin V walks hand-over-hand: Single fluorophore imaging with 1.5-nm localization. *Science* **300,** 2061–2065.

Weiss, S. (1999). Fluorescence spectroscopy of single biomolecules. *Science* **283,** 1676–1683.

Wu, X., Liu, H., Liu, J., Haley, K. N., Treadway, J. A., Larson, J. P., Ge, N., Peale, F., and Bruchez, M. P. (2003). Immunofluorescent labeling of cancer marker Her2 and other cellular targets with semiconductor quantum dots. *Nature Biotechnol.* **21,** 41–46.

[13] Development and Application of Automatic High-Resolution Light Microscopy for Cell-Based Screens

By YAEL PARAN, IRENA LAVELIN, SUHA NAFFAR-ABU-AMARA, SABINA WINOGRAD-KATZ, YUVALAL LIRON, BENJAMIN GEIGER, and ZVI KAM

Abstract

Large-scale microscopy-based screens offer compelling advantages for assessing the effects of genetic and pharmacological modulations on a wide variety of cellular features. However, development of such assays is often confronted by an apparent conflict between the need for high throughput, which usually provides limited information on a large number of samples, and a high-content approach, providing detailed information on each sample. This chapter describes a novel high-resolution screening (HRS) platform that is able to acquire large sets of data at a high rate and light microscope resolution using specific ''reporter cells,'' cultured in multiwell plates. To harvest extensive morphological and molecular information in these automated screens, we have constructed a general analysis pipeline that is capable of assigning scores to multiparameter-based comparisons between treated cells and controls. This chapter demonstrates the structure of this system and its application for several research projects, including screening of chemical compound libraries for their effect on cell adhesion, discovery of novel cytoskeletal genes, discovery of cell migration-related genes, and a siRNA screen for perturbation of cell adhesion.

METHODS IN ENZYMOLOGY, VOL. 414 0076-6879/06 $35.00

DOI: 10.1016/S0076-6879(06)14013-6